MACH REFLECTION OF WEAK SHOCK WAVES FROM A RIGID WALL

B. I. Zaslavskii and R. A. Safarov

UDC 533.6.011.72:532.593

On the basis of experimental observations and theoretical analysis of flow structure in the neighborhood of the triple point, it is shown that one should reject the condition for equality of the angle of deflection of flows passing through the Mach front and the two other fronts and replace it with some supplementary condition. The system of consistency equations in the indicated region is closed by an equation which is obtained under the assumption of the extremality of the deflection angle of a flow passing through the incident and reflected fronts. Calculations of the pressure drops behind the shock fronts agree with experimental data in this case.

1. The relations characterizing the reflection of weak shock waves from a rigid wall have been studied rather completely within the confines of the acoustic approximation [1]. For large angles of incidence, the results of this work can be extrapolated to the case of waves of small but finite amplitude.

At small angles the linear acoustic approximation is qualitatively incorrect. As has been shown [2, 3], the theory of small perturbations leads in this and similar cases to nonlinear equations for short waves with nonlinear boundary conditions. Within the framework of the theory of short waves, the problems of regular reflection and almost-grazing incidence were considered where the reflected shock wave degenerates into a weak discontinuity [2, 4]. In the latter case, the motion can be studied by the Lighthill method [5].

The problem of Mach interaction of shock waves with relatively small but finite pressure drops at angles of incidence close to the critical angle has also been considered [2, 3]. The magnitudes of the pressure drops at shock fronts in the neighborhood of the triple point were not determined in [2-9]. Experimental papers [6-9] and review papers in [10, 11] are concerned with this problem.

This paper presents the results of an experimental study with a shock tube, using optical methods, of Mach reflection of weak shock waves from a rigid wall over a broad range of angles and relative intensities along with some theoretical relations which were obtained from the consistency condition at the shock fronts.

Let a plane shock wave be incident on a wedge with an opening half-angle α. The angle between the normal to the reflected shock front at the point of intersection of the shock waves and the surface of the wedge is called the angle of reflection β and α is the angle of incidence. Regular reflection occurs for angles α greater than a certain critical angle α^*. One can establish a relation between α, β, and the intensities of the incident and reflected shock waves, $\Delta P_1 = P_1 - P_0$ and $\Delta P_2 = P_2 - P_0$, at their point of intersection. Here, P_0 is the initial pressure; P_1 and P_2 are the pressures behind the incident and reflected shock fronts.

Simple approximate formulas were obtained for this case [2]. A ratio of the pressure drops at the point of intersection of the shock fronts $\Delta P_2/\Delta P_1 \approx 3$ corresponds to the critical angle. When $\alpha < \alpha^*$, a third, Mach shock wave arises which connects the point of intersection of the incident and reflected shock waves with the rigid wall. We superimpose the origin O of a cylindrical coordinate system r, φ on the angle of the wedge and measure the angle φ from the surface of the wedge. If the flow is self-similar, the point of intersection A of the three shock waves must be displaced along some ray $\varphi = \chi$. The pressure

Moscow. Translated from Zhurnal Prikladnoi Mekhaniki i Tekhnicheskoi Fiziki, No. 5, pp. 26-33, September-October, 1973. Original article submitted May 14, 1973.

differential drops along the reflected wave in proportion to separation from the triple point and the reflected wave degenerates into a weak discontinuity with sufficient separation.

Let $r_1 = r_1(\varphi, t)$, $r_2 = r_2(\varphi, t)$, and $r_3 = r_3(\varphi, t)$ be the equations for the incident, reflected, and Mach shock waves. We write the equations for these fronts and the consistency conditions on them:

$$
\begin{aligned}
&dr_1 / \partial t = N_1[1 + \mathrm{tg}^2(\alpha + \varphi)]^{1/2} \\
&u_1 = q_1 \cos(\alpha + \varphi), \quad v_1 = -q_1 \sin(\alpha + \varphi) \\
&\partial r_2 / \partial t = [N_2 + q_1 \cos(\alpha + \beta)][1 + \mathrm{tg}^2(\beta - \varphi)]^{1/2} \\
&u_2 = q_2 \cos(\beta - \varphi) + q_1 \cos(\alpha + \varphi) \\
&v_2 = q_2 \sin(\beta - \varphi) - q_1 \sin(\alpha + \varphi) \\
&\partial r_3 / dt = N_3 (1 + \mathrm{tg}^2 \psi)^{1/2} \\
&u_3 = q_3 \cos\psi, \quad v_3 = -q_3 \sin\psi \\
&N_{1,3}^2 = c_0^2[1 + {}^1/{}_2(n+1)\varepsilon_{1,3}] \\
&N_2^2 = c_0^2[1 + {}^1/{}_2(n-1)\varepsilon_1 + {}^1/{}_2\,(n+1)\varepsilon_2]\,(1 + \Gamma_1)^{-1} \\
&q_{1,3}^2 = c_0^2\varepsilon_{1,3}^2[1 + {}^1/{}_2(n+1)\varepsilon_{1,3}]^{-1} \\
&q_2^2 = c_0^2(\varepsilon_2 - \varepsilon_1)^2[1 + {}^1/{}_2(n-1)\varepsilon_1 + {}^1/{}_2(n+1)\varepsilon_2]^{-1}(1 + \Gamma_1)^{-1} \\
&\Gamma_{1,3} = \varepsilon_{1,3}[1 + {}^1/{}_2(n-1)\varepsilon_{1,3}]^{-1} \\
&\Gamma_2 = \varepsilon_2(1 + n\varepsilon_1)[1 + n\varepsilon_1 + {}^1/{}_2(n-1)\varepsilon_2 + {}^1/{}_4(n^2-1)\varepsilon_1^2 + {}^1/{}_4(n-1)^2\varepsilon_1\varepsilon_2]^{-1} \\
&\varepsilon_i = (P_i - P_0)/nP_0, \quad \Gamma_i = (\rho_i - \rho_0)/\rho_0, \qquad i = 1, 2, 3
\end{aligned}
\tag{1.1}
$$

Here, φ is the angle between the normal to the Mach shock front and the direction of the radius vector; $N_{1,3}$ are the rates of propagation in the directions of the normals to the incident and Mach shock fronts; N_2 is the rate of propagation of the reflected shock front with respect to the particles by which it is propagated; q_1, q_2, and q_3 are the differential particle velocities at the corresponding shock fronts; ρ_1, ρ_2, and ρ_3 are the densities behind the corresponding fronts; ρ_0 is the initial density; u and v are the projections of the particle velocity vectors on the direction of the radius vector and perpendicular to it; t is time; c_0 is the velocity of sound; n is the adiabatic index.

At the point of intersection of the three shock waves,

$$r_1 = r_2 = r_3, \qquad P_2 = P_3 \tag{1.2}$$

The last condition is satisfied if the configuration of the shock waves is such that the flow behind the fronts is subsonic. If the flow is supersonic, centering of a rarefaction wave is possible.

Ordinarily we have for a third condition at the triple point [10] equal deflection of the flows passing through the two shock fronts, (Θ_2), and through the single (Mach) shock front (Θ_3). Since

$$\mathrm{tg}\,\theta_2 = \frac{v_2 \cos(\alpha + \varphi)}{N_1 - u_2 \cos(\alpha + \varphi)}, \quad \mathrm{tg}\,\theta_3 = \frac{v_3 \cos(\alpha + \varphi)}{N_1 - u_3 \cos(\alpha + \varphi)} \tag{1.3}$$

this condition can be written in the form

$$v_2[N_1 - u_3 \cos(\alpha + \chi)] = v_3[N_1 - u_2 \cos(\alpha + \chi)] \tag{1.4}$$

If Γ_1 or ε_1 are considerably less than one (weak shock waves), Eqs. (1.1) can be considerably simplified by expanding these equations in a series in powers of Γ_1, ε_1, or any other parameter Γ_0 characterizing the relative density or pressure drop at the incident wave front. In first approximation, Eqs. (1.1) take the form

$$
\begin{gathered}
(\partial\delta_1 / \partial\varphi^\circ)^2 = 2\delta_1 + 2\partial\delta_1 / \partial\tau - \gamma_1, \quad \nu_1 = -\gamma_1\ \partial\delta_1 / \partial\varphi^\circ \\
(\partial\delta_2 / \partial\varphi^\circ)^2 = 2\delta_2 + 2\partial\delta_2 / \partial\tau - \gamma_2 - \gamma_1, \quad \nu_2 = -(\gamma_2 - \gamma_1)\partial\delta_2 / \partial\varphi^\circ + \nu_1 \\
(\partial\delta_3 / \partial\varphi^0)^2 = 2\delta_3 + 2\partial\delta_3 / \partial\tau - \gamma_3, \quad \nu_3 = -\gamma_3\ \partial\delta_3 / \partial\varphi^\circ \\
\mu = \gamma
\end{gathered}
\tag{1.5}
$$

Here the following dimensionless coordinates and functions were introduced in accordance with [2]:

$$
\begin{aligned}
&\varphi^\circ = \varphi[{}^1/{}_2(n+1)\Gamma_0]^{-1/2}, \quad \delta = (r - c_0 t)[{}^1/{}_2(n+1)\Gamma_0 c_0 t]^{-1} \\
&\nu = v / c_0\Gamma_0[{}^1/{}_2(n+1)\Gamma_0]^{1/2}, \qquad \mu = u / c_0\Gamma_0 \\
&\gamma = \Gamma / \Gamma_0, \qquad \tau = \ln t
\end{aligned}
\tag{1.6}
$$

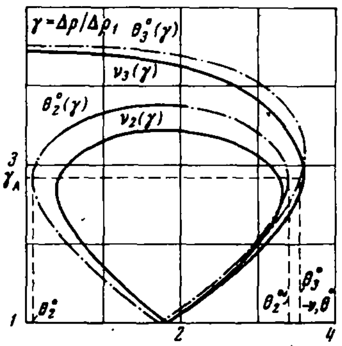

Fig. 1

Equations (1.5) are a first approximation for the expansion of Eqs. (1.1) in a series over a small parameter under the condition $\varphi \sim \Gamma_0^{1/2}$.

If the flow is explicitly independent of time, Eqs. (1.5) take the form

$$
\begin{aligned}
&d\delta_1 / d\varphi^\circ = (2\delta_1 - \gamma_1)^{1/2}, \qquad \nu_1 = -\gamma_1\, d\delta_1 / d\varphi^\circ \\
&d\delta_2 / d\varphi^\circ = \pm (2\delta_2 - \gamma_2 - \gamma_1)^{1/2}, \quad \nu_2 = -(\gamma_2 - \gamma_1)\ d\delta_2 / d\varphi^\circ + \nu_1 \\
&d\delta_3 / d\varphi^\circ = \pm (2\delta_3 - \gamma_3)^{1/2}, \qquad \nu_3 = -\gamma_3\, d\delta_3 / d\varphi^\circ
\end{aligned}
\tag{1.7}
$$

We obtain from Eqs. (1.2) and (1.4) conditions at the point A for a first approximation

$$
\delta_1 = \delta_2 = \delta_3, \qquad \gamma_2 = \gamma_3, \qquad \nu_2 = \nu_3 \tag{1.8}
$$

Since in first approximation we have at the point A

$$
\begin{aligned}
&d\delta_1 / d\varphi^\circ = b_1, \quad d\delta_2 / d\varphi^\circ = b_2, \quad d\delta_3 / d\varphi^\circ = \psi^\circ \\
&b_1 = (\alpha + \chi)[{}^1\!/_2(n+1)\Gamma_0]^{-1/2}, \quad b_2 = (\beta - \chi)[{}^1\!/_2(n+1)\Gamma_0]^{-1/2} \\
&\psi_0 = \psi[{}^1\!/_2(n+1)\Gamma_0]^{-1/2}
\end{aligned}
\tag{1.9}
$$

Eqs. (1.7) at this point are transformed to

$$
\begin{aligned}
&\nu_1 = -\gamma_1 b_1, \quad \nu_2 = \pm (\gamma_2 - \gamma_1)\ (b_1^2 - \gamma_2)^{1/2} - \gamma_1 b_1 \\
&\nu_3 = \pm \gamma_2 (b_1^2 - \gamma_2 + \gamma_1)^{1/2}, \quad b_2 = \pm (b_1^2 - \gamma_2)^{1/2} \\
&\psi^\circ = \pm (b_1^2 - \gamma_2 + \gamma_1)^{1/2}
\end{aligned}
\tag{1.10}
$$

Figure 1 shows the dependence of ν_2 and ν_3 on γ_2 in accordance with Eqs. (1.10) and the dependence of $\theta_2^\circ = \theta_2 \Gamma_0^{-1}[{}^1\!/_2 (n+1)\Gamma_0]^{-1/2}$ and $\theta_3^\circ = \theta_3 \Gamma_0^{-1}[{}^1\!/_2 (n+1)\Gamma_0]^{-1/2}$ on γ_2, which was obtained from calculations based on Eqs. (1.1) for the case $\Gamma_0 = \Gamma_1 = 0.02$. In both cases, the angle b_1 was taken to be 1.85

$$
\theta_2^\circ(\gamma_2) \to \nu_2(\gamma_2), \quad \theta_3^\circ(\gamma_2) \to \nu_3(\gamma_2) \quad \text{for} \quad \Gamma_1 \to 0
$$

It is clear from the curves shown that Eqs. (1.10) have single root $\gamma_2 = 1$ when $\Gamma_1 \to 0$ since the curves $\nu_2(\gamma_2)$ and $\nu_3(\gamma_2)$ intersect only at the initial point. The corresponding shock curves for Mach and reflected waves also intersect only at the point $\gamma_2 = 1$. Calculations show that the curves intersect only at the initial point for $\Gamma_1 \leqslant 0.2$ and for all angles of incidence corresponding to Mach reflection. This corresponds to degeneration of a reflected shock wave into a weak discontinuity.

The case where centering of a rarefaction wave occurs in the neighborhood of the triple point A (Prandtl–Meyer flow) is theoretically possible [12]. The equations for this flow in the notation (1.6) take the form [3]

$$
\begin{aligned}
&\gamma = -{}^1\!/_2\ (\delta - \delta_A)^2\ (\varphi^0 - \varphi_A^0)^{-2} + \gamma_A \\
&\nu = {}^1\!/_3\ (\delta - \delta_A)^3\ (\varphi^0 - \varphi_A^0)^{-3} + \nu_A
\end{aligned}
$$

or

$$
\gamma = -{}^1\!/_2\ [3(\nu - \nu_A)]^{2/3} + \gamma_A \tag{1.11}
$$

The slope of the characteristic with respect to a direction perpendicular to the radius vector to the point A is determined by

$$
d\delta / d\varphi^\circ = -[2\ (\delta - \gamma)]^{1/2} \tag{1.12}
$$

One easily obtains from Eqs. (1.10)-(1.12) the following expressions for the determination of all flow parameters in the neighborhood of the triple point,

$$
\begin{aligned}
&b_2 = [{}^1\!/_2\ (b_1^2 - \gamma_1)]^{1/2}, \quad \gamma_2 = {}^1\!/_2\ (b_1^2 + \gamma_1) \\
&\nu_2 = -(\gamma_2 - \gamma_1)[{}^1\!/_2(b_1^2 - \gamma_1)]^{1/2} - \gamma_1 b_1 \\
&\psi^\circ = (2\gamma_2 - \gamma_3)^{1/2}, \quad \nu_3 = -\gamma_3 \psi^\circ \\
&\gamma_3 = \gamma_2 - {}^1\!/_2[3\ (\nu_3 - \nu_2)]^{2/3}
\end{aligned}
\tag{1.13}
$$

In the neighborhood of the triple point A, $\gamma_3 < \gamma_2$; the maximum value $\gamma_A = 2.5$ is reached when $b_1 = 2$. The density drop along the reflected wave front first increases in proportion to separation from the triple point, reaching a maximum at some distance from it, and then falls.

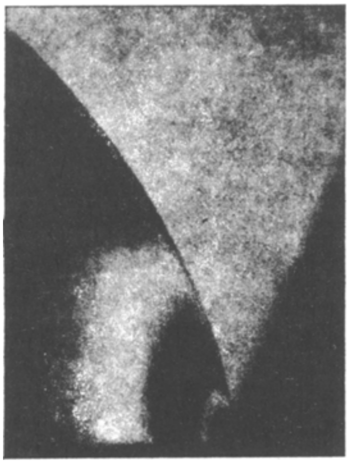

Fig. 2

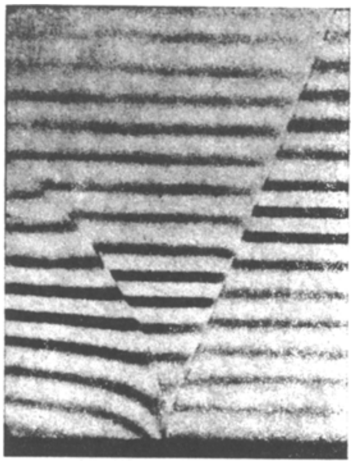

Fig. 3

2. The reflection of weak shock waves from a wedge was studied experimentally for $0.009 \leq \Gamma_1 \leq 0.132$.

The experiments were performed in a diaphragmmed shock tube with a rectangular channel 90 × 45 mm in size. In order to produce shock waves of lowest possible intensity, a high-pressure chamber was used which had a cross-sectional area five times smaller than the cross-sectional area of the channel. Between the high-pressure chamber and the channel, a transition section was installed in the form of a nozzle with a profile selected so that formation of reflected wave trains from the wall which perturb the "plug" behind the lead wave was avoided. By varying the pressure in the channel from 0.2 to 11 kg/cm^2 and the drop at the cellophane-film diaphragm from 1 to 3 kg/cm^2, we were able to vary the wave intensity over the range $0.009 < \Gamma_1 < 0.34$. The shock tube was equipped with an IAB-451 shadowgraph, an IT-42 Mach–Zender interferometer, and an SFR high-speed camera. Shadowgraphs and Schilieren photographs were taken to obtain clearer pictures of shock-wave configurations. To measure the distribution of the density drop at the shock fronts and in the flow behind them, interferograms were taken with an initial infinitely broad band and with bands of finite width.

The first kind of interferogram (Fig. 2) makes it possible to follow in detail changes in the reflection pattern during variation of the initial conditions since the interference bands correspond to lines of equal density in this case.

The second type of interferogram (Fig. 3) is suitable for obtaining numerical values of the density at any point in the field.

In calculating the reflection pattern within the confines of the short-wave theory, the basic function sought is γ (in [2, 3], it is μ; in first approximation $\mu = \gamma$).

Values of γ along the reflected and Mach fronts were measured with the help of the second kind of interferogram. The density drop $\Delta\rho$ is proportional to the band shift Δm at the corresponding point in the interferogram. If the density drop is $\Delta\rho_1$ behind the front of the incident shock wave and the band displacement on the interferogram is Δm_1, then for $\Gamma_0 = \Gamma_1$

$$\Delta\rho / \Delta\rho_1 = \Delta m / \Delta m_1 = \gamma$$

To obtain more precise data, the device was fired several times with the same wave parameters and angles α. The initial position of the interference bands varied slightly from experiment to experiment. Interference patterns were recorded in white and monochromatic light. With reliable identification of a band, this made it possible to increase the accuracy of band-shift measurement to 0.05 bands for an incident wave and to 0.1-0.3 bands for reflected and Mach waves. The error in the determination of incident-wave intensity and of the value of γ did not exceed 2 and 5% respectively.

The interferograms and shadowgrams demonstrated the self-similarity of this phenomenon. Wave configurations at various moments of time were similar. Along rays starting from the angle of the wedge, the density drop at the shock fronts during motion remained unchanged, i.e., $\gamma = \gamma(\varphi)$ for given Γ_1 and α.

Averaged curves in the γ, φ plane were constructed from an analysis of a series of interferograms for identical Γ_1 and α. The values of γ at the foot of the Mach wave (γ_B) and at the triple point (γ_A) were

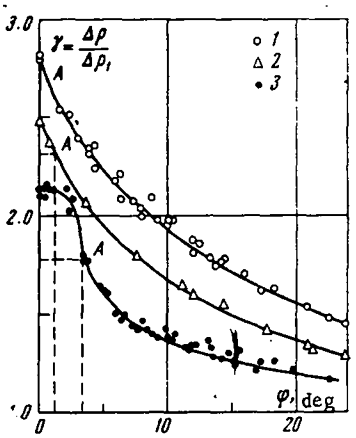

Fig. 4

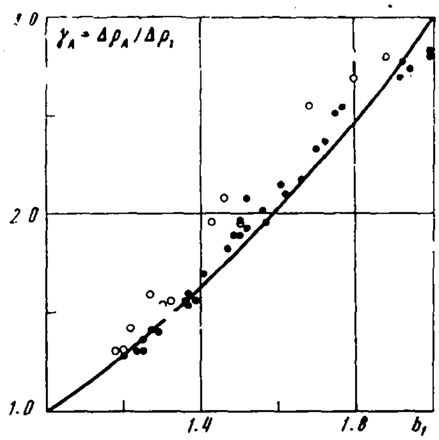

Fig. 5

were determined from the points of intersection of the resultant curve with the lines $\varphi = 0$ and χ. For example, the relation $\gamma(\varphi)$ for $\Gamma_1 = 0.132$ is shown in Fig. 4. Curve 1 was obtained for $\gamma = 32°$ ($\chi = 0$), curve 2 for $\gamma = 26.3°$ ($\chi = 1.2°$), and curve 3 for $\gamma = 20.5°$ ($\chi = 3.4°$). The position of the triple point A is shown on each curve. The maximum density drop is reached at the shock front on the surface of the wedge. The density drop along the Mach and reflected fronts, and the quantity γ corresponding to it, fall monotonically in proportion to the increase in the angle φ. At the triple point

$$\gamma_A = \gamma_A(\alpha, \Gamma_1) \quad \text{or} \quad \gamma_A = \gamma_A(\alpha + \chi, \Gamma_1)$$

When $\Gamma_1 \ll 1$, the motion can be discussed within the confines of the short-wave theory. In this case

$$\gamma_A = \gamma_A(b_1) \tag{2.1}$$

Values of $\gamma_A(b_1)$ corresponding to $0.0085 \le \Gamma_1 \le 0.022$ are indicated in Fig. 5 by open circles. The data presented indicate the density undergoes a jump at the reflected wave front even for very small values of Γ_1 and small wedge angles ($\alpha < 1/2\ \alpha^*$).

3. The facts established cannot be explained within the framework of the three-shock theory. The difficulties which arise in an attempt to explain the observed phenomena have been discussed [6, 13]. We assume that the pressure drops at the shock fronts in the neighborhood of the triple point A and the angles $\alpha + \chi$, $\beta - \chi$, and ψ associated with them take on values for which the flows passing through the incident and reflected shock fronts are deflected by the minimum possible angle. The values of ν_2 are also minimal then. The flow deflection angles Θ_2^0 and Θ_3^0 in the shock curves in Fig. 1 correspond to this mode of motion.

Under such an assumption, one can obtain in first approximation the dependence of b_1 and b_2 on γ_A

$$b_1 = [{}^1/_2(3\gamma_A - 1)]^{1/2}, \quad b_2 = [{}^1/_2(\gamma_A - 1)]^{1/2} \tag{3.1}$$

The curve $\gamma_A = \gamma_A(b_1)$ calculated from Eq. (3.1) is shown in Fig. 5. The experimental data (open circles) are to the left of this curve. With an increase in Γ_1, the points obtained from an analysis of the experimental data are shifted even more to the left. If in place of the argument

$$b_1 = (\alpha + \chi)[{}^1/_2(n+1)\Gamma_1]^{-1/2} = (\alpha + \chi)({}^1/_2\alpha^*)^{-1}$$

in Eq. (2.1), we take

$$b_{1e} = (\alpha + \chi)\,({}^1/_2\alpha_e^*)^{-1}$$

the experimental data obtained for $0.0085 \le \Gamma_1 \le 0.132$ (solid circles in Fig. 5) lie on the general curve.

Equations (3.1) are transformed to

$$\begin{aligned} \alpha + \chi &= {}^1/_2\alpha_e^*[{}^1/_2(3\gamma_A - 1)]^{1/2} \\ \beta - \chi &= {}^1/_2\alpha_e^*\,[{}^1/_2\,(\gamma_A - 1)]^{1/2} \end{aligned} \tag{3.2}$$

Here, α^* is the value of the critical angle calculated from the asymptotic expression, α_e^* is the observed value, and $\alpha^* \to \alpha_e^*$, $b_1 \to b_{1e}$ when $\Gamma_1 \to 0$. The difference between α^* and α_e^* is significant when $\Gamma_1 > 0.05$.

Thus the experiments are in agreement with Eqs. (3.2) and disagree qualitatively with the theory given in Section.1.

Apparently Eq. (1.4) is not satisfied at the triple point, i.e., in the neighborhood of that point, the velocity vectors of the particles passing through one and two shock fronts form a finite angle $\Theta_3 - \Theta_2$ in the moving coordinate system. There must be a region bounded by two tangential discontinuities where the velocity is considerably reduced and the pressure is the same as the pressure in neighboring regions. This region should be an area of intense vortex flow.

The experiment indicates (Fig. 2) there is a region in the neighborhood of the triple point where the density behind a front increased downstream and does not decrease as it does in neighboring regions. The existence of a region of "inverse" density gradients is also a confirmation of the proposed assumption since the input of mass into the angular region $(\theta_3 - \theta_2)$ is only possible with such a trend in density gradient and pressure.

Equations (3.1) were derived under assumption of the extremality of the angle of deflection of the flow passing through the two fronts. There are two such angles – a minimum θ_2° and a maximum $\theta_2^{\circ\prime}$. In both cases, the density drops at the fronts in the neighborhood of the triple point are identical. The reflection angles β for the minimum angles θ_2° are close to those observed.

The authors thank S. A. Khristianovich for consideration of the work and advice.

LITERATURE CITED

1. A. Ya. Sagomonyan, Three-Dimensional Problems in Transient Motion of Compressible Fluids [in Russian], Izd. MGU, Moscow (1962).
2. O. S. Ryzhov and S. A. Khristianovich, "Nonlinear reflection of weak shock waves," Prikl. Matem. Mekhan., 22, No. 5 (1958).
3. A. A. Grib, O. S. Ryzhov, and S. A. Khristianovich, "Theory of short waves," Zh. Prikl. Mekhan. i Tekh. Fiz., No. 1 (1960).
4. G. P. Shindyapin, "Irregular reflection of weak shock waves from a rigid wall," Zh. Prikl. Mekhan. i Tekh. Fiz., No. 2 (1964).
5. M. J. Lighthill, "The diffraction of blast. I., "Proc. Roy. Soc. (London), 198, No. 1055 (1949).
6. R. Kawamura and H. Saito, "Reflection of shock waves. I. Pseudostationary case," J. Phys. Soc., Japan, 11, No. 5 (1956).
7. C. H. Fletcher, A. H. Taub, and W. Bleakney, "The Mach reflection of shock waves at nearly glacing incidence," Rev. Mod. Phys., 23, No. 3 (1951).
8. L. G. Smith, "Photographic investigation of the reflection of plane shocks in air," Off. Sci. Res. and Develop., No. 6271 (1945).
9. W. Bleakney and A. H. Taub, "Interaction of shock waves," Rev. Mod. Phys., 21, No. 4 (1949).
10. R. Courant and K. Friedrichs, Supersonic Flow and Shock Waves, Wiley (1948).
11. T. V. Bazhenova, L. G. Gvozdeva, Yu. S. Lobastov, I. M. Naboko, R. G. Nemkov, and O. A. Predvoditeleva, Shock Waves in Real Gases [in Russian], Nauka, Moscow (1968).
12. K. G. Gooderly, Theory of Near-Sonic Flow [Russian translation], Izd. Inostr. Lit., Moscow (1960).
13. J. Sternberg, "Triple-shock-wave intersections," Phys. Fluids, 2, No. 2 (1959).